
ATTRACTOR STATES OF THE FUNCTIONAL BRAIN CONNECTOME ORCHESTRATE LARGE-SCALE BRAIN DYNAMICS

Robert Englert

Balint Kincses

Raviteja Kotikalapudi

Giuseppe Gallitto

Jialin Li

Kevin Hoffschlag

Choong-Wan Woo

Tor D. Wager

Dagmar Timmann

Ulrike Bingel

 **Tamas Spisak¹**

Wednesday 1st November, 2023

Abstract

¹Correspondence to: tamas.spisak@uk-essen.de

Understanding large-scale brain dynamics is a grand challenge in neuroscience. We propose functional connectome-based Hopfield neural networks (fcHNNs) as a model of macro-scale brain dynamics, arising from recurrent activity flow among brain regions. An fcHNN is neither optimized to mimic certain brain characteristics, nor trained to solve specific tasks; its weights are simply initialized with empirical functional connectivity values. In the fcHNN framework, brain dynamics are understood in relation to so-called attractor states, i.e. neurobiologically meaningful low-energy activity configurations. Analyses of 7 distinct datasets demonstrate that fcHNNs can accurately reconstruct and predict brain dynamics under a wide range of conditions, including resting and task states and brain disorders. By establishing a mechanistic link between connectivity and activity, fcHNNs offers a simple and interpretable computational alternative to conventional descriptive analyses of brain function. Being a generative framework, fcHNNs can yield mechanistic insights and hold potential to uncover novel treatment targets.

Keywords

Key Points:

- We present a simple yet powerful computational model for large-scale brain dynamics
- The model uses a functional connectome-based Hopfield artificial neural network (fcHNN) architecture to compute recurrent "activity flow" through the functional brain connectome
- FcHNNs accurately reconstruct the dynamic repertoire of the brain in resting conditions
- FcHNNs conceptualize both task-induced and pathological changes in brain activity as a non-linear shift in these dynamics
- Our approach is validated using data from seven studies involving approximately 1000 participants

0.1 Introduction

Brain function is characterized by the continuous activation and deactivation of anatomically distributed neuronal populations [Buzsaki, 2006]. Irrespective of the presence or absence of explicit stimuli, brain regions appear to work in concert, giving rise to a rich and spatiotemporally complex fluctuation [Bassett and Sporns, 2017]. This fluctuation is neither random, nor stationary over time [Liu and Duyn, 2013, Zalesky et al., 2014]. It is organized around large-scale gradients [Margulies et al., 2016, Huntenburg et al., 2018] and exhibits quasi-periodic properties, with a limited number of recurring patterns known as "brain states" [Greene et al., 2023, Vidaurre et al., 2017, Liu and Duyn, 2013].

A wide variety of descriptive techniques have been previously employed to characterize whole-brain dynamics [Smith et al., 2012, Vidaurre et al., 2017, Liu and Duyn, 2013, Chen et al., 2018]. These efforts have provided accumulating evidence not only for the existence of dynamic brain states but also for their clinical significance [Hutchison et al., 2013, Barttfeld et al., 2015, Meer et al., 2020]. However, the underlying driving forces remain elusive due to the descriptive nature of such studies.

Conventional computational approaches attempt to solve this puzzle by going all the way down to the biophysical properties of single neurons, and aim to construct a model of larger neural populations, or even the entire brain [Breakspear, 2017]. These approaches have shown numerous successful applications [Murray et al., 2018, Kriegeskorte and Douglas, 2018, Heinz et al., 2019]. However, the estimation of the vast number of free parameters in such models hampers their ability to effectively bridge the gap between explanations at the level of single neurons and the complexity of behavior [Breakspear, 2017]. Recent efforts using coarse-grained brain network models [Schirner et al., 2022, Schiff et al., 1994, Papadopoulos et al., 2017] and linear network control theory [Chiêm et al., 2021, Scheid et al., 2021, Gu et al., 2015] opted to trade biophysical fidelity to phenomenological validity. The challenge for such models lies in modelling the relation between the structural wiring of the brain and functional connectivity. The "neuroconnectionist" approach, on the other hand, [Doerig et al., 2023] aims at "cognitive/behavioral fidelity" [Kriegeskorte and Douglas, 2018], by using artificial neural networks (ANNs) that are trained to perform various tasks, as brain models. However, the need to train ANNs for specific tasks inherently limits their ability to explain task-independent, spontaneous neural dynamics [Richards et al., 2019].

Here we propose a novel approach that combines the advantages of large-scale network models and neuroconnectionism, to investigate brain dynamics. Similar to neuroconnectionism, we utilize an ANN as a high-level computational model of the brain. However, our model is not explicitly trained for a specific task. Instead,

we set its weights empirically, with data based on the "activity flow" [Cole et al., 2016, Ito et al., 2017] across regions within the functional brain connectome, as measured with functional magnetic resonance imaging (fMRI, Figure 0.1B).

Specifically, we employ a continuous-space Hopfield neural network (HNN) [Hopfield, 1982, Krotov, 2023], with its nodes representing large-scale brain areas, and its weights initialized with the functional connectivity values between these areas. Based on the topology of the functional connectome, this architecture establishes an energy level for any arbitrary activation patterns and determines a "trajectory of least action" towards one of the finite number of stable patterns, known as *attractor states*, that minimize this energy. In this simplistic yet powerful framework, brain dynamics can be conceptualized as an intricate, high-dimensional path on the energy landscape (Figure 0.1C), arising from the activity flow [Cole et al., 2016] within the functional connectome and constrained by the "gravitational pull" of the attractor states of the system. Given its generative nature, the proposed model offers testable predictions for the effect of various perturbations and alterations of these dynamics, from task-induced activity, to changes related to brain disorders.

In the present work, we use HNNs to explore the functional connectome's attractor-dynamics with the aid of a streamlined, low-dimensional representation of the energy landscape. Subsequently, we use a diverse set of experimental, clinical and meta-analytic studies to evaluate our model's ability to reconstruct various characteristics of resting state brain dynamics, as well as its capacity to detect and explain changes induced by experimental tasks or alterations in brain disorders.

0.2 Results

0.2.1 Connectome-based Hopfield network as a model of brain dynamics

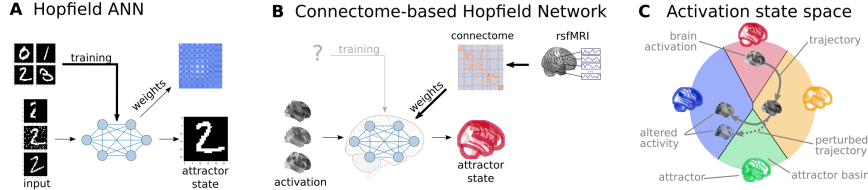
First, we explored the attractor states of the functional connectome in a sample of $n=41$ healthy young participants (Table ??). We estimated interregional activity flow [Cole et al., 2016, Ito et al., 2017] as the study-level average of regularized partial correlations among the resting state fMRI timeseries of $m = 122$ functionally defined brain regions (see Methods for details). We then used the standardized functional connectome as the w_{ij} weights of a fully connected recurrent ANN, specifically a continuous-state Hopfield network [Hopfield, 1982, Koiran, 1994] consisting of m neural units, each having an activity $a_i \in [-1, 1] \subset \mathbb{R}$). Hopfield networks can be initialized by an arbitrary activation pattern (consisting of m activation values) and iteratively updated (i.e. "relaxed") until their energy converges a local minimum, that is, to one of the finite number of attractor states (see Methods). The relaxation procedure is based on a simple rule; in each iteration, the activity of a region is constructed as the weighted average of the activities of all other regions, with weights defined by the connectivity between them. The average is then transformed by a sigmoidal activation function, to keep it in the desired $[-1, 1]$ interval. This can be expressed by the following equation:

$$\dot{a}_i = S(\beta \sum_{j=1}^m w_{ij} a_j - b_i) \quad (1)$$

where \dot{a}_i is the activity of neural unit i in the next iteration and $S(a_j)$ is the sigmoidal activation function ($S(a) = \tanh(a)$ in our implementation) and b_i is the bias of unit i and β is the so-called temperature parameter. For the sake of simplicity, we set $b_i = 0$ in all our experiments. We refer to this architecture as a functional connectivity-based Hopfield Neural Network (fcHNN). The relaxation of a fcHNN model can be conceptualized as the repeated application of the activity flow principle [Cole et al., 2016, Ito et al., 2017], simultaneously for all regions: $\dot{a}_i = \sum_{j=1}^m w_{ij} a_j$. The update rule also exhibits analogies with network control theory [Gu et al., 2015] and the inner workings of neural mass models, as applied e.g. in dynamic causal modeling [Daunizeau et al., 2012].

Hopfield networks assign an energy value to each possible activity configuration [Hopfield, 1982, Koiran, 1994], which decreases during the relaxation procedure until reaching an equilibrium state with minimal energy (Figure 0.2.1A, top panel). We used a large number of random initializations to obtain all possible attractor states of the connectome-based Hopfield network in study 1 (Figure 0.2.1A, bottom panel).

Consistent with theoretical expectations, we observed that increasing the temperature parameter β led to an increasing number of attractor states (Figure 0.2.1E, left, Figure ??), appearing in symmetric pairs (i.e. $a_i^{(1)} = -a_i^{(2)}$). For simplicity, we set the temperature parameter for the rest of the paper to a value resulting in 4 distinct attractor states ($\beta = 0.4$).



A Hopfield artificial neural networks (HNNs) are a form of recurrent artificial neural networks that serve as content-addressable ("associative") memory systems. Hopfield networks can be trained to store a finite number of patterns (e.g. via Hebbian learning a.k.a. "fire together - wire together"). During the training procedure, the weights of the HNN are trained so that the stored patterns become stable attractor states of the network. Thus, when the trained network is presented partial, noisy or corrupted variations of the stored patterns, it can effectively reconstruct the original pattern via an iterative relaxation procedure that converges to the attractor states. **B** We consider regions of the brain as nodes of a Hopfield network.

Instead of training the Hopfield network to specific tasks, we set its weights empirically, with the interregional activity flow estimated via functional brain connectivity. Capitalizing on strong analogies between the relaxation rule of Hopfield networks and the activity flow principle that links activity to connectivity in brain networks, we propose the resulting functional connectome-based Hopfield neural network (fcHNN) as a computational model for macro-scale brain dynamics.

C The proposed computational framework assigns an energy level, an attractor state and a position in a low-dimensional embedding to brain activation patterns. Additionally, it models how the entire state-space of viable activation patterns is restricted by the dynamics of the system and how alterations in activity and/or connectivity modify these dynamics.

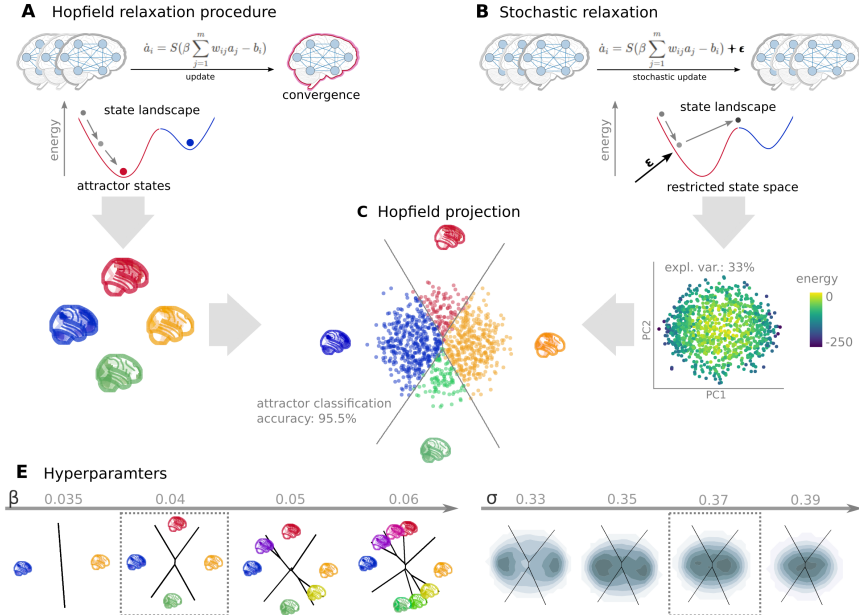
A Hopfield artificial neural networks (HNNs) are a form of recurrent artificial neural networks that serve as content-addressable ("associative") memory systems. Hopfield networks can be trained to store a finite number of patterns (e.g. via Hebbian learning a.k.a. "fire together - wire together"). During the training procedure, the weights of the HNN are trained so that the stored patterns become stable attractor states of the network. Thus, when the trained network is presented partial, noisy or corrupted variations of the stored patterns, it can effectively reconstruct the original pattern via an iterative relaxation procedure that converges to the attractor states. **B** We consider regions of the brain as nodes of a Hopfield network. Instead of training the Hopfield network to specific tasks, we set its weights empirically, with the interregional activity flow estimated via functional brain connectivity. Capitalizing on strong analogies between the relaxation rule of Hopfield networks and the activity flow principle that links activity to connectivity in brain networks, we propose the resulting functional connectome-based Hopfield neural network (fcHNN) as a computational model for macro-scale brain dynamics.

C The proposed computational framework assigns an energy level, an attractor state and a position in a low-dimensional embedding to brain activation patterns. Additionally, it models how the entire state-space of viable activation patterns is restricted by the dynamics of the system and how alterations in activity and/or connectivity modify these dynamics.

Figure 1: **Connectome-based Hopfield networks as models of macro-scale brain dynamics.**

A Hopfield artificial neural networks (HNNs) are a form of recurrent artificial neural networks that serve as content-addressable ("associative") memory systems. Hopfield networks can be trained to store a finite number of patterns (e.g. via Hebbian learning a.k.a. "fire together - wire together"). During the training procedure, the weights of the HNN are trained so that the stored patterns become stable attractor states of the network. Thus, when the trained network is presented partial, noisy or corrupted variations of the stored patterns, it can effectively reconstruct the original pattern via an iterative relaxation procedure that converges to the attractor states. **B** We consider regions of the brain as nodes of a Hopfield network. Instead of training the Hopfield network to specific tasks, we set its weights empirically, with the interregional activity flow estimated via functional brain connectivity. Capitalizing on strong analogies between the relaxation rule of Hopfield networks and the activity flow principle that links activity to connectivity in brain networks, we propose the resulting functional connectome-based Hopfield neural network (fcHNN) as a computational model for macro-scale brain dynamics.

C The proposed computational framework assigns an energy level, an attractor state and a position in a low-dimensional embedding to brain activation patterns. Additionally, it models how the entire state-space of viable activation patterns is restricted by the dynamics of the system and how alterations in activity and/or connectivity modify these dynamics.



A Top: During so-called relaxation procedure, activities in the nodes of an fCHNN model are iteratively updated based on the activity of all other regions and the connectivity between them. The energy of a connectome-based Hopfield network decreases during the relaxation procedure until reaching an equilibrium state with minimal energy, i.e. an attractor state. Bottom: Four attractor states of the CHNN derived from the group-level functional connectivity matrix from Table ?? ($n=44$). **B** Top: Similarly to stochastic dynamic causal modeling, in presence of weak noise (stochastic update), the system does not converge to equilibrium anymore. Instead, activity transverses on the state landscape in a way restricted by the topology of the connectome and the "gravitational pull" of the attractor states. Bottom: We sample the state space by running the stochastic relaxation procedure for an extended amount of time (e.g. 100.000 consecutive stochastic updates), each point representing a possible activation configuration (state).

To construct a low-dimensional representation of the state space, we take the first two principal components of the simulated activity patterns. The first two principal components explain approximately 58-85% of the variance of state energy (depending on the noise parameter σ , see Figure ??). **C** We map all states of the state space sample to their corresponding attractor state, with the conventional Hopfield relaxation procedure (A). The four attractor states are also visualized in their corresponding position on the PCA-based projection. The first two principal components yield a clear separation of the attractive state basins (cross-validated classification accuracy: 95.5%, Figure ??). We refer to the resulting visualization as the fCHNN projection and use it to visualize fCHNN-derived and empirical brain dynamics throughout the rest of the manuscript. **E** At its simplest form, the fCHNN framework entails only two free hyperparameters: the temperature parameter β (left) that controls the number of attractor states and the noise parameter of the stochastic relaxation σ . To avoid overfitting these parameters to the empirical data, we set $\beta = 0.04$ and $\sigma = 0.37$ for the rest of the paper (dotted boxes).

A Top: During so-called relaxation procedure, activities in the nodes of an fCHNN model are iteratively updated based on the activity of all other regions and the connectivity between them. The energy of a connectome-based Hopfield network decreases during the relaxation procedure until reaching an equilibrium state with minimal energy, i.e. an attractor state. Bottom: Four attractor states of the CHNN derived from the group-level functional connectivity matrix from Table ?? ($n=44$). **B** Top: Similarly to stochastic dynamic causal modeling, in presence of weak noise (stochastic update), the system does not converge to equilibrium anymore. Instead, activity transverses on the state landscape in a way restricted by the topology of the connectome and the "gravitational pull" of the attractor states. Bottom: We sample the state space by running the stochastic relaxation procedure for an extended amount of time (e.g. 100.000 consecutive stochastic updates), each point representing a possible activation configuration (state). To construct a low-dimensional representation of the state space, we take the first two principal components of the simulated activity patterns. The first two principal components explain approximately 58-85% of the variance of state energy (depending on the noise parameter σ , see Figure ??). **C** We map all states of the state space sample to their corresponding attractor state, with the conventional Hopfield relaxation procedure (A). The four attractor states are also visualized in their corresponding position on the PCA-based projection. The first two principal components yield a clear separation of the attractive state basins (cross-validated classification accuracy: 95.5%, Figure ??). We refer to the resulting visualization as the fCHNN projection and use it to visualize fCHNN-derived and empirical brain dynamics throughout the rest of the manuscript. **E** At its simplest form, the fCHNN framework entails only two free hyperparameters: the temperature parameter β (left) that controls the number of attractor states and the noise parameter of the stochastic relaxation σ . To avoid overfitting these parameters to the empirical data, we set $\beta = 0.04$ and $\sigma = 0.37$ for the rest of the paper (dotted boxes).

FcHNNs, without any modifications, always converge to an equilibrium state. To incorporate stochastic fluctuations in neuronal activity [Robinson et al., 2005], we introduced weak Gaussian noise to the fcHNN relaxation procedure. This procedure, referred to as stochastic relaxation, prevents the system from reaching equilibrium and, somewhat similarly to stochastic DCM [Daunizeau et al., 2012], induces complex system dynamics (Figure 0.2.1B).

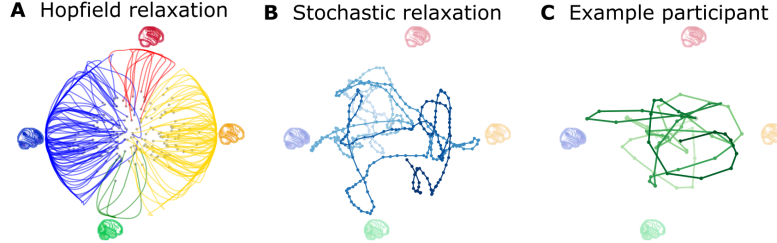
In order to enhance interpretability, we obtained the first two principal components (PCs) of the states sampled from stochastic relaxation procedure. The resulting two-dimensional embedding (Figure 0.2.1B, bottom plot) exhibited high consistency across different values of β and σ (Figure 0.2.1E). For all subsequent analyses, we set $\sigma = 0.37$ (based a coarse optimization procedure aimed at reconstructing the bimodal distribution of empirical data, Figure 0.2.1E right). On the low-dimensional embedding, which we refer to as the *fcHNN projection*, we observed a clear separation of the attractor states (Figure 0.2.1C), with the two symmetric pairs of attractor states located at the extremes of the first and second PC. To map the attractor basins on the space spanned by the first two PCs (Figure 0.2.1C), we obtained the attractor state of each point visited during the stochastic relaxation and fit a multinomial logistic regression model to predict the attractor state from the first two PCs. The resulting model accurately predicted attractor states of arbitrary brain activity patterns, achieving a cross-validated accuracy of 96.5%. The attractor basins were visualized by using the decision boundaries obtained from this model. (Figure 0.2.1C). We propose the 2-dimensional fcHNN projection depicted on (Figure 0.2.1C) as a simplified representation of brain dynamics, and use it as a basis for all subsequent analyses in this work. Examples are presented on Figure 0.2.1.

0.2.2 Reconstruction of resting state brain dynamics

The spatial patterns of the obtained attractor states exhibit high neuroscientific relevance and closely resemble previously described large-scale brain systems. (Figure 0.2.2A). The first pair of attractors (mapped on PC1, horizontal axis) resemble the two complementary "macro" systems described, among others, by Golland et al. [2008] and Cioli et al. [2014] as well as the two "primary" brain states observed by Chen et al. [2018] and the 'unimodal to transmodal' principal gradient of Margulies et al. [2016] and Huntenburg et al. [2018]. A common interpretation of these two patterns is that they represent (i) an "extrinsic" system linked to the immediate sensory environment and (ii) an "intrinsic" system for higher-level internal context. The other pair of attractors spans an orthogonal axis, and resemble to patterns commonly associated with perception-action cycles [Fuster, 2004], and described as a gradient across sensory-motor modalities [Huntenburg et al., 2018], recruiting regions associated with active inference (e.g. motor cortices) and perceptual inference (e.g. visual areas).

The discovered attractor states demonstrate remarkable replicability (mean Pearson's correlation 0.93) across the discovery dataset (study 1) and two independent replication datasets (Table ??, Figure 0.2.2C). Moreover, they were found to be robust to noise added to the connectome ({numref}`Supplementary Figure %s <si_noise_robustness_weights>`).

Further analysis in study 1 showed that connectome-based Hopfield models accurately reconstructed multiple characteristics of true resting-state data. First, the first two components of the fcHNN projection accounted for a substantial amount of variance in the real resting-state fMRI data in study 1 (mean $R^2 = 0.399$) and generalized well to out-of-sample data (study 2, mean $R^2 = 0.396$) (Figure 0.2.2E). Remarkably, the explained variance of the fcHNN projection significantly exceeded that of a PCA performed directly on the real resting-state fMRI data itself ($R^2 = 0.37$ and 0.364 for in- and out-of-sample analyses). Second, fcHNN analyses accurately reconstructed true resting brain state dynamics. During stochastic relaxation, the fcHNN model was found to spend approximately three-quarters of the time on the basis of the first two attractor states and one-quarter on the basis of the second pair of attractor states (approximately equally distributed between pairs). We observed strikingly similar temporal occupancies in the real data (Figure 0.2.2D), statistically significant with various null models (Figure ??). Fine-grained details of the bimodal distribution observed in the real resting-state fMRI data were also convincingly reproduced by the fcHNN model (Figure 0.2.2F and Figure 0.2.1E). Finally, fcHNNs were found to generate signal that preserves the covariance structure of the real functional connectome, indicating that dynamic systems of this type (including the brain) inevitably "leak" their underlying structure into the activity time series, strengthening the construct validity of our approach (Figure 0.2.2D).



A The fcHNN of study 1 seeded with real activation maps (gray dots) of an example participant. All activation maps converge to one of the four attractor states during the relaxation procedure (without noise). Trajectories are colored by attractor state. **B** Illustration of the stochastic relaxation procedure in the same fcHNN model. The system does not converge to an attractor state but instead transverses the state space in a way restricted by the topology of the connectome and the "gravitational pull" of the attractor states. The shade of the trajectory changes with increasing number of iterations. The trajectory is smoothed with a moving average over 10 iterations for visualization purposes. **C** Real resting state fMRI data of an example participant from study 1, plotted on the fcHNN projection. The shade of the trajectory changes with increasing number of iterations.

A The fcHNN of study 1 seeded with real activation maps (gray dots) of an example participant. All activation maps converge to one of the four attractor states during the relaxation procedure (without noise). Trajectories are colored by attractor state. **B** Illustration of the stochastic relaxation procedure in the same fcHNN model. The system does not converge to an attractor state but instead transverses the state space in a way restricted by the topology of the connectome and the "gravitational pull" of the attractor states. The shade of the trajectory changes with increasing number of iterations. The trajectory is smoothed with a moving average over 10 iterations for visualization purposes. **C** Real resting state fMRI data of an example participant from study 1, plotted on the fcHNN projection. The shade of the trajectory changes with increasing number of iterations.

Figure 3: **Examples trajectories on the fcHNN projection.**

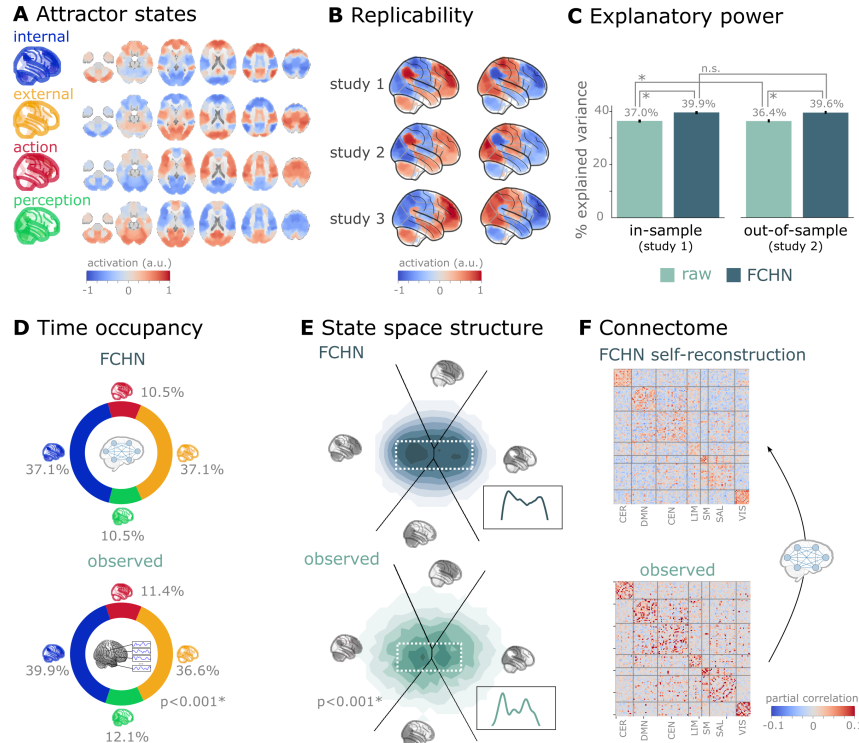
A The fcHNN of study 1 seeded with real activation maps (gray dots) of an example participant. All activation maps converge to one of the four attractor states during the relaxation procedure (without noise). Trajectories are colored by attractor state. **B** Illustration of the stochastic relaxation procedure in the same fcHNN model. The system does not converge to an attractor state but instead transverses the state space in a way restricted by the topology of the connectome and the "gravitational pull" of the attractor states. The shade of the trajectory changes with increasing number of iterations. The trajectory is smoothed with a moving average over 10 iterations for visualization purposes. **C** Real resting state fMRI data of an example participant from study 1, plotted on the fcHNN projection. The shade of the trajectory changes with increasing number of iterations.

0.2.3 An explanatory framework for task-based brain activity

Next to reproducing various characteristics of spontaneous brain dynamics, fcHNNs can also be used to model responses to various perturbations. We obtained task-based fMRI data from a study by [Woo et al. \[2015\]](#) (Table ??, n=33, see Figure 0.2.2), investigating the neural correlates of pain and its self-regulation.

We found that activity changes due to pain (taking into account hemodynamics, see Methods) were characterized on the fcHNN projection by a shift towards the attractor state of action-execution (permutation test for mean projection difference by randomly swapping conditions, $p < 0.001$, Figure 0.2.3A, left). Energies, as defined by the fcHNN, were also significantly different between the two conditions ($p < 0.001$), with higher energies during pain stimulation.

When participants were instructed to up- or downregulate their pain sensation (resulting in increased and decreased pain reports and differential brain activity in the nucleus accumbens, NAc (see [Woo et al. \[2015\]](#) for details)), we observed further changes of the location of momentary brain activity patterns on the fcHNN projection ($p < 0.001$, Figure 0.2.3A, right), with down-regulation pulling brain dynamics towards the attractor state of internal context and perception. Interestingly, self-regulation did not trigger significant energy changes ($p = 0.36$).

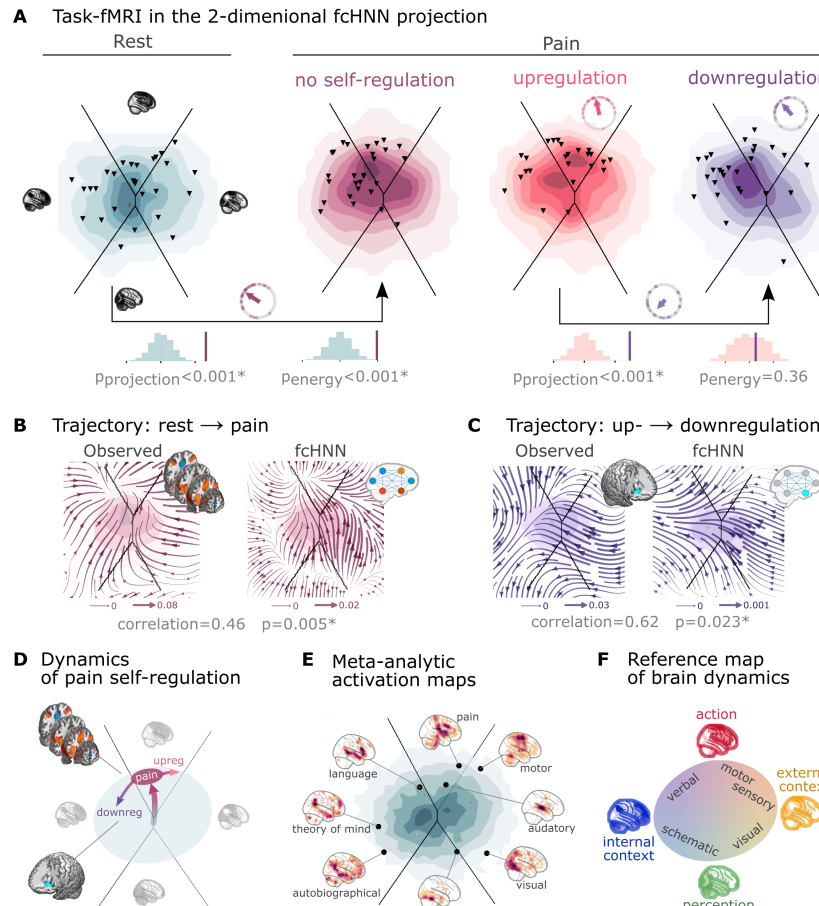


A The four attractor states of the fcHNN model from study 1 reflect brain activation patterns with high neuroscientific relevance, representing sub-systems previously associated with 'internal context' (blue), "external context" (yellow), "action/execution" (red) and "perception" (green) [Golland et al., 2008, Cioli et al., 2014, Chen et al., 2018, Fuster, 2004, Margulies et al., 2016]. **B** The attractor states show excellent replicability in two external datasets (study 2 and 3, mean correlation 0.93). **C** The fcHNN projection (first two PCs of the fcHNN state space) explains significantly more variance ($p<0.0001$) in the real resting state fMRI data than principal components derived from the real resting state data itself and generalizes better ($p<0.0001$) to out-of-sample data (study 2). Error bars denote 99% bootstrapped confidence intervals. **D** The fcHNN analysis accurately predicts ($p<0.0001$) the fraction of time spent on the basis of the four attractor states in real resting state fMRI data (study 1) and, **E**, reconstructs the characteristic bimodal distribution of the real resting state data. **F** Stochastic fcHNNs are capable of self-reconstruction: the timeseries resulting from the stochastic relaxation procedure mirror the co-variance structure of the functional connectome the fcHNN model was initialized with.

A The four attractor states of the fcHNN model from study 1 reflect brain activation patterns with high neuroscientific relevance, representing sub-systems previously associated with 'internal context' (blue), "external context" (yellow), "action/execution" (red) and "perception" (green) [Golland et al., 2008, Cioli et al., 2014, Chen et al., 2018, Fuster, 2004, Margulies et al., 2016]. **B** The attractor states show excellent replicability in two external datasets (study 2 and 3, mean correlation 0.93). **C** The fcHNN projection (first two PCs of the fcHNN state space) explains significantly more variance ($p<0.0001$) in the real resting state fMRI data than principal components derived from the real resting state data itself and generalizes better ($p<0.0001$) to out-of-sample data (study 2). Error bars denote 99% bootstrapped confidence intervals. **D** The fcHNN analysis accurately predicts ($p<0.0001$) the fraction of time spent on the basis of the four attractor states in real resting state fMRI data (study 1) and, **E**, reconstructs the characteristic bimodal distribution of the real resting state data. **F** Stochastic fcHNNs are capable of self-reconstruction: the timeseries resulting from the stochastic relaxation procedure mirror the co-variance structure of the functional connectome the fcHNN model was initialized with.

Figure 4: **Connectome-based Hopfield networks reconstruct characteristics of real resting state brain activity.**

A The four attractor states of the fcHNN model from study 1 reflect brain activation patterns with high neuroscientific relevance, representing sub-systems previously associated with 'internal context' (blue), "external context" (yellow), "action/execution" (red) and "perception" (green) [Golland et al., 2008, Cioli et al., 2014, Chen et al., 2018, Fuster, 2004, Margulies et al., 2016]. **B** The attractor states show excellent replicability in two external datasets (study 2 and 3, mean correlation 0.93). **C** The fcHNN projection (first two PCs of the fcHNN state space) explains significantly more variance ($p<0.0001$) in the real resting state fMRI data than principal components derived from the real resting state data itself and generalizes better ($p<0.0001$) to out-of-sample data (study 2). Error bars denote 99% bootstrapped confidence intervals. **D** The fcHNN analysis accurately predicts ($p<0.0001$) the fraction of time spent on the basis of the four attractor states in real resting state fMRI data (study 1) and, **E**, reconstructs the characteristic bimodal distribution of the real resting state data. **F** Stochastic fcHNNs are capable of self-reconstruction: the timeseries resulting from the stochastic relaxation procedure mirror the co-variance structure of the functional connectome the fcHNN model was initialized with.



A Functional MRI time-frames during pain stimulation from Table ?? (second fcHNN projection plot) and self-regulation (third and fourth) are distributed differently on the fcHNN projection than brain states during rest (first projection, permutation test, $p<0.001$ for all). Energies, as defined by the Hopfield model, are also significantly different between rest and the pain conditions (permutation test, $p<0.001$), with higher energies during pain stimulation. Triangles denote participant-level mean activations in the various blocks (corrected for hemodynamics). Small circle plots show the directions of the change for each individual (points) as well as the mean direction across participants (arrow), as compared to the reference state (downregulation for the last circle plot, rest for all other circle plots). **B** Flow-analysis (difference in the average timeframe-to-timeframe transition direction) reveals a non-linear difference in brain dynamics during pain and rest (left). When introducing weak pain-related signal in the fcHNN model during stochastic relaxation, it accurately reproduces these non-linear flow differences (right). **C** Simulating activity in the Nucleus Accumbens (NAc) (the region showing significant activity differences in Woo et al. [2015]) reconstructs the observed non-linear flow difference between up- and downregulation (left). **D** Schematic representation of brain dynamics during pain and its up- and downregulation, visualized on the fcHNN projection. In the proposed framework, pain does not simply elicit a direct response in certain regions, but instead, shifts spontaneous brain dynamics towards the "action" attractor, converging to a characteristic "ghost attractor" of pain. Down-regulation by NAc activation exerts force towards the attractor of internal context, leading to the brain less frequent "visiting" pain-associated states. **E** Visualizing meta-analytic activation maps on the fcHNN projection captures intimate relations between the corresponding tasks and **F** serves as a basis for a fcHNN-based theoretical interpretative framework for spontaneous and task-based brain dynamics. In the proposed framework, task-based activity is not a mere response to external stimuli in certain brain locations but a perturbation of the brain's characteristic dynamic trajectories, constrained by the underlying functional connectivity. From this perspective, "activity maps" from conventional task-based fMRI analyses capture time-averaged differences in these whole brain dynamics.

A Functional MRI time-frames during pain stimulation from Table ?? (second fcHNN projection plot) and self-regulation (third and fourth) are distributed differently on the fcHNN projection than brain states during rest (first projection, permutation test, $p<0.001$ for all). Energies, as defined by the Hopfield model, are also significantly different between rest and the pain conditions (permutation test, $p<0.001$), with higher energies during pain stimulation. Triangles denote participant-level mean activations in the various blocks (corrected for hemodynamics). Small circle plots show the directions of the change for each individual (points) as well as the mean direction across participants (arrow), as compared to the reference state (downregulation for the last circle plot, rest for all other circle plots). **B** Flow-analysis (difference in the average timeframe-to-

Next, we conducted a "flow analysis" on the fcHNN projection, quantifying how the average timeframe-to-timeframe transition direction differs on the fcHNN projection between conditions (see Methods). This analysis unveiled that during pain (Figure 0.2.3B, left side), brain activity tends to gravitate towards a distinct point on the projection, which we term the "ghost attractor" of pain (similar to Vohryzek et al. [2020]). On the boundary the basins of the internal and action attractors. In case of downregulation (as compared to upregulation), brain activity is pulled away from the pain-related "ghost attractor" (Figure 0.2.3C, left side), towards the attractor of internal context.

Our fcHNN was able to accurately reconstruct these non-linear dynamics by adding a small amount of realistic "control signal" (similarly to network control theory Liu et al. [2011], Gu et al. [2015]). To simulate the alterations in brain dynamics during pain stimulation, we acquired a meta-analytic pain activation map [Zunhammer et al., 2021] ($n=603$) and incorporated it as a control signal added to each iteration of the stochastic relaxation procedure. The ghost attractor found in the empirical data was present across a relatively wide range of signal-to-noise (SNR) values (Figure ??). Results with SNR=0.005 are presented on Figure 0.2.3B, right side (Pearson's $r = 0.46$, $p=0.005$ based on randomizing conditions on a per-participant basis).

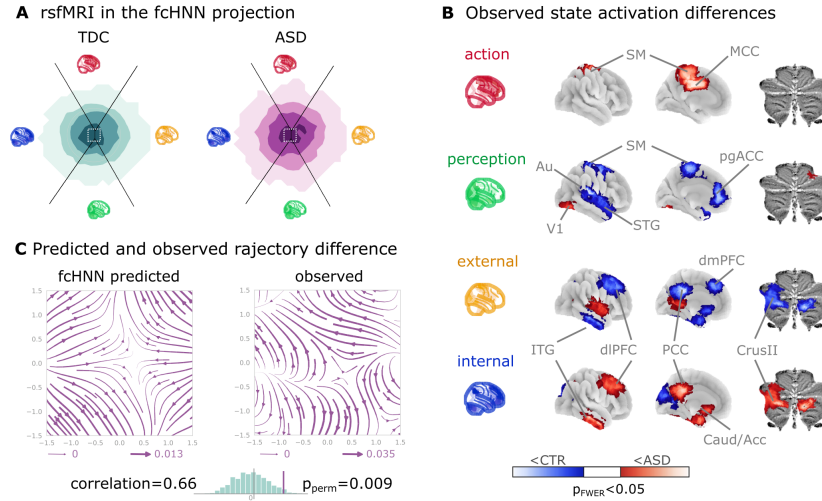
The same model was also able to reconstruct the observed non-linear differences in brain dynamics between the up- and downregulation conditions (Pearson's $r = 0.62$, $p=0.023$) without any further optimization (SNR=0.005, Figure 0.2.3C, right side). The only change we made to the model was the addition (downregulation) or subtraction (upregulation) of control signal in the NAc (the region in which [Woo et al., 2015] observed significant changes between up- and downregulation), introducing a signal difference of $\Delta\text{SNR}=0.005$ (the same value we found optimal in the pain-analysis). Results were reproducible with lower NAc SNRs, too (Figure ??).

To provide a comprehensive picture on how tasks and stimuli other than pain map onto the fcHNN projection, we obtained various task-based meta-analytic activation maps from Neurosynth (see Methods) and plotted them on the fcHNN projection (Figure 0.2.3E). This analysis reinforced and extended our interpretation of the four investigated attractor states and shed more light on how various functions are mapped on the axes of internal vs. external context and perception vs. action. In the coordinate system of the fcHNN projection, visual processing is labeled "external-perception", sensory-motor processes "external-active", language, verbal cognition and working memory is labelled "internal-active" and long-term memory as well as social and autobiographic schemata fall into the "internal-perception" regime (Figure 0.2.3F).

0.2.4 Clinical relevance

We obtained data from $n=172$ autism spectrum disorder (ASD) and typically developing control (TDC) individuals, acquired at the New York University Langone Medical Center, New York, NY, USA (NYU) and generously shared in the Autism Brain Imaging Data Exchange dataset (Table ???: ABIDE, [Di Martino et al., 2014]). After excluding high-motion cases (see Methods), we visualized the distribution of time-frames on the fcHNN-projection separately for the ASD and TDC groups (Figure 0.2.4A). First, we assigned all timeframes to one of the 4 attractor states with the fcHNN from study 1 and found several significant differences in the mean activity on the attractor basins (see Methods) of the ASD group as compared to the respective controls (Figure 0.2.4B). Strongest differences were found on the "action-perception" axis (Table 1), with increased activity of the sensory-motor and middle cingulate cortices during "action-execution" related states and increased visual and decreased sensory and auditory activity during "perception" states, likely reflecting the widely acknowledged, yet poorly understood, perceptual atypicalities in ASD [Hadad and Schwartz, 2019]. ASD related changes in the internal-external axis were characterized by more involvement of the posterior cingulate, the precuneus, the nucleus accumbens, the dorsolateral prefrontal cortex (dlPFC), the cerebellum (Crus II, lobule VII) and inferior temporal regions during activity of the internalizing subsystem (Table 1). While similar, default mode network (DMN)-related changes have often been attributed to an atypical integration of information about the "self" and the "other" [Padmanabhan et al., 2017], a more detailed fcHNN-analysis may help to further disentangle the specific nature of these changes.

Thus, we contrasted the characteristic trajectories derived from the fcHNN models of the two groups (initialized with the group-level functional connectomes). Our FcHNN-based flow analysis predicted that in ASD, there is an increased likelihood of states returning towards the middle from the internal-external axis and an increased likelihood of states transitioning towards the extremes of the action-perception axis (Figure 0.2.4C). We observed a highly similar pattern in the real data (Pearson's correlation: 0.66), statistically significant after permutation testing (shuffling the group assignment, $p=0.009$).



A The distribution of time-frames on the fcHNN-projection separately for ASD patients and typically developing control (TDC) participants.

B We quantified attractor state activations in the Autism Brain Imaging Data Exchange datasets (Table ??) as the individual-level mean activation of all time-frames belonging to the same attractor state.

This analysis captured alterations similar to those previously associated to ASD-related perceptual atypicalities (visual, auditory and somatosensory cortices) as well as atypical integration of information about the “self” and the “other” (default mode network regions). All results are corrected for multiple comparisons across brain regions and attractor states (122*4 comparisons) with Bonferroni-correction. See Table 1 and Figure ?? for detailed results.

C The comparison of data generated by fcHNNs initialized with ASD and TDC connectomes, respectively, revealed a characteristic pattern of differences in the system’s dynamics, with increased pull towards (and potentially a higher separation between) the action and perception attractors attractors and a lower tendency of trajectories going towards the internal and external attractors.

Abbreviations: MCC: middle cingulate cortex, ACC: anterior cingulate cortex, pg: perigenual, PFC: prefrontal cortex, dm: dorsomedial, dl: dorsolateral, STG: superior temporal gyrus, ITG: inferior temporal gyrus, Caud/Acc: caudate-accumbens, SM: sensorimotor, V1: primary visual, A1: primary auditory, SMA: supplementary motor cortex, ASD: autism spectrum disorder, TDC: typically developing control.

A The distribution of time-frames on the fcHNN-projection separately for ASD patients and typically developing control (TDC) participants.

B We quantified attractor state activations in the Autism Brain Imaging Data Exchange datasets (Table ??) as the individual-level mean activation of all time-frames belonging to the same attractor state. This analysis captured alterations similar to those previously associated to ASD-related perceptual atypicalities (visual, auditory and somatosensory cortices) as well as atypical integration of information about the “self” and the “other” (default mode network regions). All results are corrected for multiple comparisons across brain regions and attractor states (122*4 comparisons) with Bonferroni-correction. See Table 1 and Figure ?? for detailed results.

C The comparison of data generated by fcHNNs initialized with ASD and TDC connectomes, respectively, revealed a characteristic pattern of differences in the system’s dynamics, with increased pull towards (and potentially a higher separation between) the action and perception attractors attractors and a lower tendency of trajectories going towards the internal and external attractors.

Abbreviations: MCC: middle cingulate cortex, ACC: anterior cingulate cortex, pg: perigenual, PFC: prefrontal cortex, dm: dorsomedial, dl: dorsolateral, STG: superior temporal gyrus, ITG: inferior temporal gyrus, Caud/Acc: caudate-accumbens, SM: sensorimotor, V1: primary visual, A1: primary auditory, SMA: supplementary motor cortex, ASD: autism spectrum disorder, TDC: typically developing control.

Figure 6: Connectome-based Hopfield analysis of autism spectrum disorder.

A The distribution of time-frames on the fcHNN-projection separately for ASD patients and typically developing control (TDC) participants.

B We quantified attractor state activations in the Autism Brain Imaging Data Exchange datasets (Table ??)

Table 1: The top ten largest changes in average attractor-state activity between autistic and control individuals. Mean attractor-state activity changes are presented in the order of their absolute effect size. All p-values are based on permutation tests (shuffling the group assignment) and corrected for multiple comparisons (via Bonferroni's correction). For a comprehensive list of significant findings, see {numref}`Supplementary Figure %s <si_clinical_results_table>`.

region	attractor	effect size	p-value
primary auditory cortex	perception	-0.126	<0.0001
middle cingulate cortex	action	0.109	<0.0001
cerebellum lobule VIIb (medial part)	internal context	0.104	<0.0001
mediolateral sensorimo- tor cortex	perception	-0.099	0.00976
precuneus	action	0.098	<0.0001
middle superior tempo- ral gyrus	perception	-0.098	<0.0001
frontal eye field	perception	-0.095	<0.0001
dorsolateral sensorimo- tor cortex	perception	-0.094	0.00976
posterior cingulate cor- tex	action	0.092	<0.0001
dorsolateral prefrontal cortex	external context	-0.092	<0.0001

0.3 Discussion

In this study, we have introduced and validated a simple yet robust computational generative framework that elucidates how activity propagation within the functional connectome orchestrates large-scale brain dynamics, leading to the spontaneous emergence of brain states and characteristic dynamic responses to perturbations.

The construct validity of our model is rooted in the activity flow principle, first introduced by Cole et al. [2016]. The activity flow principle states that activity in a brain region can be predicted by a weighted combination of the activity of all other regions, where the weights are set to the functional connectivity of those regions to the held-out region. This principle has been shown to hold across a wide range of experimental and clinical conditions [Cole et al., 2016, Ito et al., 2017, Mill et al., 2022, Hearne et al., 2021, Chen et al., 2018]. The proposed approach is based on the intuition that the repeated, iterative application of the activity flow equation in a system exhibits close analogies with a type of recurrent artificial neural networks known as Hopfield networks [Hopfield, 1982].

Hopfield networks have been widely acknowledged for their relevance for brain function, including the ability to store and recall memories [Hopfield, 1982], self-repair [Murre et al., 2003], a staggering robustness to noisy or corrupted inputs [Hertz et al., 1991] (see also Figure ??) and the ability to produce multistable dynamics organized by the "gravitational pull" of a finite number of attractor states [Khona and Fiete, 2022]. While many of such properties of Hopfield networks have previously been proposed as a model for micro-scale neural systems (see Khona and Fiete [2022] for a review), the proposed link between macro-scale activity propagation and Hopfield networks allows transferring the vast body of knowledge on Hopfield networks to the study of large-scale brain dynamics.

Integrating Cole's activity flow principle with the HNN architecture mandates the initiation of network weights with functional connectivity values, specifically partial correlations as suggested by Cole et al. [2016]. Considering the functional connectome as weights of an already trained neural network distinguishes our methodology not only from conventional biophysical and phenomenological computational modeling strategies, which usually rely on the structural connectome as a proxy for polysynaptic connectivity [Cabral et al., 2017], but also from "neuroconnectionist" approaches that employ explicit training procedures [Doerig et al., 2023].

As compared to finely detailed biophysical models with many free parameters, the basic form of the fcHNN approach comprises solely two "hyperparameters" (temperature and noise) and yields notably consistent outcomes across an extensive range of these parameters (Figure ??, Figure ??, Figure ??, Figure ??)).

To underscore the potency of this simplicity and stability, in the present work, we avoided any unnecessary parameter optimization. It is likely, however, that extensive parameter optimization could further improve the performance of the model.

Another advantage of fcHNNs over more detailed models is that fcHNNs establish a simple and easily interpretable link between two highly prevalent metrics of brain function: functional connectivity and brain activity. This connection is not solely phenomenological, but also mathematical, facilitating the exploration and prediction of alterations in the system's dynamics in response to perturbations affecting both activity and connectivity.

The proposed model also exhibits several advantages over linear network control theory-based [Gu et al., 2015] approaches. First, the fcHNN approach works with direct activity flow estimates and does not require knowledge about the structural-functional coupling in the brain. Second, the fcHNN approach is based on a non-linear ANN architecture, thus, similarly to neuroconnectionist approaches, allows leveraging on knowledge about the ANN architecture itself. Specifically, the fcHNNs provide a mechanistic account for the emergence of large-scale canonical brain networks [Zalesky et al., 2014] and brain states or the presence of "ghost attractors" [Deco and Jirsa, 2012, Vohryzek et al., 2020], via the key concept in the Hopfield network framework, the attractor states.

In comparison to conventional neuroconnectionist approaches, fcHNNs do not need to be trained to solve tasks and thus allow for the exploration of spontaneous brain dynamics. However, it is worth mentioning that, like any other ANNs, fcHNNs can also be further trained via established ANN training techniques (e.g. via the Hebbian learning rule) to "solve" various tasks or to match altered dynamics during development or in clinical populations. In this interesting future direction, the training procedure itself becomes part of the model, providing testable hypotheses about the formation, and various malformations, of brain dynamics.

Given its simplicity, it is remarkable, if not surprising, how accurately the fcHNN model is able to reconstruct and predict brain dynamics under a wide range of conditions. Particularly interesting is the result that the two-dimensional fcHNN projection can explain more variance in real resting state fMRI data than the first two principal components derived from the data itself. A plausible explanation for the remarkable reconstruction performance is that, through their known noise tolerance, fcHNNs are able to capture essential principles of the underlying dynamic processes even if our empirical measurements are corrupted by noise and low sampling rate. Indeed, fcHNN attractor states were found to be robust to noisy weights (Figure ??) and highly replicable across datasets acquired at different sites, with different scanners and imaging sequences (study 2 and 3). The observed level of replicability allowed us to re-use the fcHNN model constructed with the connectome of study 1 for all subsequent analyses, without any further fine-tuning or study-specific parameter optimization.

Conceptually, the notion of a global attractor model of the brain network is not new [Deco and Jirsa, 2012]. The present work suggests, however, that the brain as an attractor network necessarily 'leaks' its code in form of the partial correlation across the regional timeseries, allowing us to uncover its large-scale attractor states. Moreover, we demonstrate that the brain's attractor states are not solely local minima in the state-space but act as a driving force for the dynamic trajectories of brain activity. Nevertheless, attractor states should not be confused with the conventional notion of brain states (e.g. co-activation patterns [Chen et al., 2015]). In the fcHNN framework, attractor states can rather be conceptualized as "Platonic idealizations" of brain activity, that are continuously approximated - but never reached - by the brain, resulting in a complex, clustered distribution of actual brain activation, with re-occurring patterns.

Relying on previous work, we can establish a relatively straightforward (although somewhat speculative) correspondence between attractor states and brain function, mapping brain activation on the axes of internal vs. external context [Golland et al., 2008, Cioli et al., 2014], as well as perception vs. action [Fuster, 2004]. This four-attractor architecture exhibits an appealing analogy with Friston's free energy principle [Friston et al., 2006] that postulate the necessary existence of subsystems for active and perceptual inference as well as a hierarchically organized (i.e. external and internal) subsystems that give rise to consciousness [Ramstead et al., 2023, Lee et al., 2023].

Both conceptually and in terms of analysis practices, resting and task states are often treated as separate phenomena. However, in the fcHNN framework, the differentiation between task and resting states is considered an artificial dichotomy. Task-based brain activity in the fcHNN framework is not a mere response to external stimuli in certain brain locations but a perturbation of the brain's characteristic dynamic trajectories, with increased preference for certain locations on the energy landscape ("ghost attractors"). In our analyses, the fcHNN approach captures and predicts participant-level activity changes induced by pain and

its self-regulation and gave a mechanistic account for how relatively small activity changes in a single region (NAcc) may result in a significantly altered pain experience.

Brain dynamics can not only be perturbed by task or other types of experimental or naturalistic interventions, but also by pathological alterations. Here we have demonstrated (study 7) that fcHNN-based analyses can characterize and predict altered brain dynamics in autism spectrum disorder (ASD). The observed ASD-associated changes in brain dynamics are indicative of a reduced ability to flexibly switch between internal and external modes of processing, corroborating previous findings that ASD sensory-driven connectivity transitions do not converge to transmodal areas [Hong et al., 2019]. Such findings are in line with previous reports of a reduced influence of context on the interpretation of incoming sensory information in ASD (e.g. the violation of Weber's law) [Hadad and Schwartz, 2019].

Together, our findings open up a series of exciting opportunities for the better understanding of brain function in health and disease.

First, the 2-dimensional fcHNN projection offers a streamlined framework not only for the visualization, but also for the *interpretation*, of brain activity patterns, as it conceptualizes changes related to various behavioral or clinical states or traits as a shift in brain dynamics in relation to brain attractor states.

Second, fcHNN analyses may provide insights into the causes of changes in brain dynamics, by for instance, identifying the regions or connections that act as an "Achilles heel" in generating such changes. Such analyses could, for instance, aid the differentiation of primary causes and secondary effects of particular activity or connectivity changes in various clinical conditions.

Third, the fcHNN approach can provide testable predictions about the effects of pharmacological interventions as well as non-invasive brain stimulation (e.g. transcranial magnetic or direct current stimulation, focused ultrasound, etc) and neurofeedback. Obtaining the optimal stimulation or treatment target within the fcHNN framework (e.g. by means of network control theory [Liu et al., 2011]) is one of the most promising future directions with the potential to significantly advance the development of novel, personalized treatment approaches.

In this initial work, we presented the simplest possible implementation of the fcHNN concept. It is clear that the presented analyses exploit only a small proportion of the richness of the full state-space dynamics reconstructed by the fcHNN model. There are many potential ways to further improve the utility of the fcHNN approach. Increasing the number of reconstructed attractor states (by increasing the temperature parameter), investigating higher-dimensional dynamics, fine-tuning the hyperparameters, testing the effect of different initializations and perturbations are all important directions for future work, with the potential to further improve the model's accuracy and usefulness.

0.4 Conclusion

To conclude, here we have proposed a lightweight, high-level computational framework that accurately captures and predicts brain dynamics under a wide range of conditions. The framework models large-scale activity flow in the brain with a recurrent artificial neural network architecture that, instead of being trained to solve specific tasks or mimic certain dynamics, is simply initialized with the empirical functional connectome. The framework identifies neurobiologically meaningful attractor states and provides a model for how these restrict brain dynamics. The proposed framework, referred to as the connectome-based Hopfield neural network (fcHNN) model, can accurately reconstruct and predict brain dynamics under a wide range of conditions, including resting state, task-induced activity changes, as well as brain disorders. FcHNNs establish a conceptual link between connectivity and activity and offer a simple, robust, and highly interpretable computational alternative to conventional descriptive approaches to investigating brain function. The generative nature of the proposed model opens up a series of exciting opportunities for future research, including predicting the effect, and understanding the mechanistic bases, of various interventions; thereby paving the way for designing novel treatment approaches.

0.5 Acknowledgements

The work was supported by the Deutsche Forschungsgemeinschaft (DFG, German Research Foundation; projects 'TRR289 - Treatment Expectation', ID 422744262 and 'SFB1280 - Extinction Learning', ID 316803389) and by IBS-R015-D1 (Institute for Basic Science; C.W.-W.).

0.6 Analysis source code

<https://github.com/pni-lab/connattractor>

0.7 Project website

<https://pni-lab.github.io/connattractor/>

0.8 Data availability

Study 1,2 and 4 is available at openneuro.org (ds002608, ds002608, ds000140). Data for study 3 is available upon request. Data for study 5-6 is available at the github page of the project: <https://github.com/pni-lab/connattractor>. Study 7 is available at https://fcon_1000.projects.nitrc.org/indi/abide/, preprocessed data is available at <http://preprocessed-connectomes-project.org/>.

References

- Gyorgy Buzsaki. *Rhythms of the Brain*. Oxford university press, 2006.
- Danielle S Bassett and Olaf Sporns. Network neuroscience. *Nature neuroscience*, 20(3):353–364, 2017.
- Xiao Liu and Jeff H Duyn. Time-varying functional network information extracted from brief instances of spontaneous brain activity. *Proceedings of the National Academy of Sciences*, 110(11):4392–4397, 2013.
- Andrew Zalesky, Alex Fornito, Luca Cocchi, Leonardo L Gollo, and Michael Breakspear. Time-resolved resting-state brain networks. *Proceedings of the National Academy of Sciences*, 111(28):10341–10346, 2014.
- Daniel S Margulies, Satrajit S Ghosh, Alexandros Goulas, Marcel Falkiewicz, Julia M Huntenburg, Georg Langs, Gleb Bezgin, Simon B Eickhoff, F Xavier Castellanos, Michael Petrides, et al. Situating the default-mode network along a principal gradient of macroscale cortical organization. *Proceedings of the National Academy of Sciences*, 113(44):12574–12579, 2016.
- Julia M Huntenburg, Pierre-Louis Bazin, and Daniel S Margulies. Large-scale gradients in human cortical organization. *Trends in cognitive sciences*, 22(1):21–31, 2018.
- Abigail S Greene, Corey Horien, Daniel Barson, Dustin Scheinost, and R Todd Constable. Why is everyone talking about brain state? *Trends in Neurosciences*, 2023.
- Diego Vidaurre, Stephen M Smith, and Mark W Woolrich. Brain network dynamics are hierarchically organized in time. *Proceedings of the National Academy of Sciences*, 114(48):12827–12832, 2017.
- Stephen M Smith, Karla L Miller, Steen Moeller, Junqian Xu, Edward J Auerbach, Mark W Woolrich, Christian F Beckmann, Mark Jenkinson, Jesper Andersson, Matthew F Glasser, et al. Temporally-independent functional modes of spontaneous brain activity. *Proceedings of the National Academy of Sciences*, 109(8):3131–3136, 2012.
- Richard H Chen, Takuya Ito, Kaustubh R Kulkarni, and Michael W Cole. The human brain traverses a common activation-pattern state space across task and rest. *Brain Connectivity*, 8(7):429–443, 2018.
- R Matthew Hutchison, Thilo Womelsdorf, Elena A Allen, Peter A Bandettini, Vince D Calhoun, Maurizio Corbetta, Stefania Della Penna, Jeff H Duyn, Gary H Glover, Javier Gonzalez-Castillo, et al. Dynamic functional connectivity: promise, issues, and interpretations. *Neuroimage*, 80:360–378, 2013.
- Pablo Barttfeld, Lynn Uhrig, Jacobo D Sitt, Mariano Sigman, Béchir Jarraya, and Stanislas Dehaene. Signature of consciousness in the dynamics of resting-state brain activity. *Proceedings of the National Academy of Sciences*, 112(3):887–892, 2015.
- Johan N van der Meer, Michael Breakspear, Luke J Chang, Saurabh Sonkusare, and Luca Cocchi. Movie viewing elicits rich and reliable brain state dynamics. *Nature communications*, 11(1):5004, 2020.
- Michael Breakspear. Dynamic models of large-scale brain activity. *Nature neuroscience*, 20(3):340–352, 2017.
- John D Murray, Murat Demirtaş, and Alan Anticevic. Biophysical modeling of large-scale brain dynamics and applications for computational psychiatry. *Biological Psychiatry: Cognitive Neuroscience and Neuroimaging*, 3(9):777–787, 2018.
- Nikolaus Kriegeskorte and Pamela K Douglas. Cognitive computational neuroscience. *Nature neuroscience*, 21(9):1148–1160, 2018.

- Andreas Heinz, Graham K Murray, Florian Schlagenhauf, Philipp Sterzer, Anthony A Grace, and James A Waltz. Towards a unifying cognitive, neurophysiological, and computational neuroscience account of schizophrenia. *Schizophrenia bulletin*, 45(5):1092–1100, 2019.
- Michael Schirner, Xiaolu Kong, BT Thomas Yeo, Gustavo Deco, and Petra Ritter. Dynamic primitives of brain network interaction. *NeuroImage*, 250:118928, 2022.
- Steven J Schiff, Kristin Jerger, Duc H Duong, Taeun Chang, Mark L Spano, and William L Ditto. Controlling chaos in the brain. *Nature*, 370(6491):615–620, 1994.
- Lia Papadopoulos, Jason Z Kim, Jürgen Kurths, and Danielle S Bassett. Development of structural correlations and synchronization from adaptive rewiring in networks of kuramoto oscillators. *Chaos: An Interdisciplinary Journal of Nonlinear Science*, 27(7), 2017.
- Benjamin Chiêm, Frédéric Crevecoeur, and Jean-Charles Delvenne. Structure-informed functional connectivity driven by identifiable and state-specific control regions. *Network Neuroscience*, 5(2):591–613, 2021.
- Brittany H Scheid, Arian Ashourvan, Jennifer Stiso, Kathryn A Davis, Fadi Mikhail, Fabio Pasqualetti, Brian Litt, and Danielle S Bassett. Time-evolving controllability of effective connectivity networks during seizure progression. *Proceedings of the National Academy of Sciences*, 118(5):e2006436118, 2021.
- Shi Gu, Fabio Pasqualetti, Matthew Cieslak, Qawi K Telesford, Alfred B Yu, Ari E Kahn, John D Medaglia, Jean M Vettel, Michael B Miller, Scott T Grafton, et al. Controllability of structural brain networks. *Nature communications*, 6(1):8414, 2015.
- Adrien Doerig, Rowan P Sommers, Katja Seeliger, Blake Richards, Jenann Ismael, Grace W Lindsay, Konrad P Kording, Talia Konkle, Marcel AJ Van Gerven, Nikolaus Kriegeskorte, et al. The neuroconnectionist research programme. *Nature Reviews Neuroscience*, pages 1–20, 2023.
- Blake A Richards, Timothy P Lillicrap, Philippe Beaudoin, Yoshua Bengio, Rafal Bogacz, Amelia Christensen, Claudia Clopath, Rui Ponte Costa, Archy de Berker, Surya Ganguli, et al. A deep learning framework for neuroscience. *Nature neuroscience*, 22(11):1761–1770, 2019.
- Michael W Cole, Takuya Ito, Danielle S Bassett, and Douglas H Schultz. Activity flow over resting-state networks shapes cognitive task activations. *Nature neuroscience*, 19(12):1718–1726, 2016.
- Takuya Ito, Kaustubh R Kulkarni, Douglas H Schultz, Ravi D Mill, Richard H Chen, Levi I Solomyak, and Michael W Cole. Cognitive task information is transferred between brain regions via resting-state network topology. *Nature communications*, 8(1):1027, 2017.
- John J Hopfield. Neural networks and physical systems with emergent collective computational abilities. *Proceedings of the national academy of sciences*, 79(8):2554–2558, 1982.
- Dmitry Krotov. A new frontier for hopfield networks. *Nature Reviews Physics*, pages 1–2, 2023.
- Pascal Koiran. Dynamics of discrete time, continuous state hopfield networks. *Neural Computation*, 6(3): 459–468, 1994.
- Jean Daunizeau, Klaas Enno Stephan, and Karl J Friston. Stochastic dynamic causal modelling of fmri data: should we care about neural noise? *Neuroimage*, 62(1):464–481, 2012.
- Peter A Robinson, CJ Rennie, Donald L Rowe, SC O'Connor, Gordon, and E. Multiscale brain modelling. *Philosophical Transactions of the Royal Society B: Biological Sciences*, 360(1457):1043–1050, 2005.
- Yulia Golland, Polina Golland, Shlomo Bentin, and Rafael Malach. Data-driven clustering reveals a fundamental subdivision of the human cortex into two global systems. *Neuropsychologia*, 46(2):540–553, 2008.
- Claudia Cioli, Hervé Abdi, Derek Beaton, Yves Burnod, and Salma Mesmoudi. Differences in human cortical gene expression match the temporal properties of large-scale functional networks. *PloS one*, 9(12):e115913, 2014.
- Joaquin M Fuster. Upper processing stages of the perception–action cycle. *Trends in cognitive sciences*, 8 (4):143–145, 2004.
- Choong-Wan Woo, Mathieu Roy, Jason T Buhle, and Tor D Wager. Distinct brain systems mediate the effects of nociceptive input and self-regulation on pain. *PLoS biology*, 13(1):e1002036, 2015.
- Jakub Vohryzek, Gustavo Deco, Bruno Cessac, Morten L Kringelbach, and Joana Cabral. Ghost attractors in spontaneous brain activity: Recurrent excursions into functionally-relevant bold phase-locking states. *Frontiers in systems neuroscience*, 14:20, 2020.
- Yang-Yu Liu, Jean-Jacques Slotine, and Albert-László Barabási. Controllability of complex networks. *nature*, 473(7346):167–173, 2011.

- Matthias Zunhammer, Tamás Spisák, Tor D Wager, and Ulrike Bingel. Meta-analysis of neural systems underlying placebo analgesia from individual participant fmri data. *Nature communications*, 12(1):1391, 2021.
- Adriana Di Martino, Chao-Gan Yan, Qingyang Li, Erin Denio, Francisco X Castellanos, Kaat Alaerts, Jeffrey S Anderson, Michal Assaf, Susan Y Bookheimer, Mirella Dapretto, et al. The autism brain imaging data exchange: towards a large-scale evaluation of the intrinsic brain architecture in autism. *Molecular psychiatry*, 19(6):659–667, 2014.
- Bat-Sheva Hadad and Sivan Schwartz. Perception in autism does not adhere to webers law. *Elife*, 8:e42223, 2019.
- Aarthi Padmanabhan, Charles J Lynch, Marie Schaer, and Vinod Menon. The default mode network in autism. *Biological Psychiatry: Cognitive Neuroscience and Neuroimaging*, 2(6):476–486, 2017.
- Ravi D Mill, Julia L Hamilton, Emily C Winfield, Nicole Lalta, Richard H Chen, and Michael W Cole. Network modeling of dynamic brain interactions predicts emergence of neural information that supports human cognitive behavior. *PLoS Biology*, 20(8):e3001686, 2022.
- Luke J Hearne, Ravi D Mill, Brian P Keane, Grega Repovš, Alan Anticevic, and Michael W Cole. Activity flow underlying abnormalities in brain activations and cognition in schizophrenia. *Science advances*, 7(29):eabf2513, 2021.
- Jaap MJ Murre, Robert Griffioen, and IH Robertson. Selfrepairing neural networks: a model for recovery from brain damage. In *Knowledge-Based Intelligent Information and Engineering Systems: 7th International Conference, KES 2003, Oxford, UK, September 2003. Proceedings, Part II* 7, pages 1164–1171. Springer, 2003.
- John Hertz, Andres Krogh, and Richard G Palmer. Introduction to the theory of neural computation, chapter 7. *Lecture Notes*, 1, 1991.
- Mikail Khona and Ila R Fiete. Attractor and integrator networks in the brain. *Nature Reviews Neuroscience*, 23(12):744–766, 2022.
- Joana Cabral, Morten L Kringelbach, and Gustavo Deco. Functional connectivity dynamically evolves on multiple time-scales over a static structural connectome: Models and mechanisms. *NeuroImage*, 160:84–96, 2017.
- Gustavo Deco and Viktor K Jirsa. Ongoing cortical activity at rest: criticality, multistability, and ghost attractors. *Journal of Neuroscience*, 32(10):3366–3375, 2012.
- Jingyuan E Chen, Catie Chang, Michael D Greicius, and Gary H Glover. Introducing co-activation pattern metrics to quantify spontaneous brain network dynamics. *Neuroimage*, 111:476–488, 2015.
- Karl Friston, James Kilner, and Lee Harrison. A free energy principle for the brain. *Journal of physiology-Paris*, 100(1-3):70–87, 2006.
- Maxwell JD Ramstead, Mahault Albarracin, Alex Kiefer, Brennan Klein, Chris Fields, Karl Friston, and Adam Safron. The inner screen model of consciousness: applying the free energy principle directly to the study of conscious experience. *arXiv preprint arXiv:2305.02205*, 2023.
- Sungwoo Lee, Younghyun Oh, Hyunhoe An, Hyebhin Yoon, Karl J Friston, Seok Jun Hong, and Choong-Wan Woo. Life-inspired interoceptive artificial intelligence for autonomous and adaptive agents. *arXiv preprint arXiv:2309.05999*, 2023.
- Seok-Jun Hong, Reinder Vos de Wael, Richard AI Bethlehem, Sara Lariviere, Casey Paquola, Sofie L Valk, Michael P Milham, Adriana Di Martino, Daniel S Margulies, Jonathan Smallwood, et al. Atypical functional connectome hierarchy in autism. *Nature communications*, 10(1):1022, 2019.